JOURNAL OF MATERIALS SCIENCE 12 (1977) 2291–2302

Creep of polycrystalline alumina, pure and doped with transition metal impurities

PAUL A. LESSING*, RONALD S. GORDON
Department of Materials Science and Engineering, University of Utah, Salt Lake City, Utah, USA

Grain size effects were used to evaluate the relative contributions of aluminium lattice and oxygen grain boundary diffusion to the high temperature (1350 to 1550° C) steady state creep of polycrystalline alumina, pure and doped with transition metal impurities (Cr, Fe). Divalent iron in solid solution was found to enhance both aluminium lattice and oxygen grain-boundary diffusion. Large concentrations of divalent iron led to viscous Coble creep which was rate-limited entirely by oxygen grain-boundary diffusion. Nabarro–Herring creep which was rate-limited by aluminium lattice diffusion was observed in pure and chromium-doped material. Chromium additions had no effect on diffusional creep rates but significantly depressed non-viscous creep modes of deformation. Creep deformation maps were constructed at various iron dopant concentrations to illustrate the relative contributions of aluminium grain boundary, aluminium lattice, and oxygen grain-boundary diffusion to the diffusional creep of polycrystalline alumina.

1. Introduction

Hollenberg and Gordon [1] have shown that either a divalent (Fe^{2+}) or quadrivalent (Ti^{4+}) impurity in solid solution in increasing amounts enhances the creep rate of polycrystalline alumina over the creep rate of pure and chromium-doped material of the same grain size. These conclusions were drawn from experiments in which the effect of oxygen partial pressure on the steady state creep rate $\dot{\epsilon}$ was studied. Increasing the oxygen partial pressure enhanced the creep rate of titanium-doped, depressed the creep rate of iron-doped, and had no effect on the creep of chromium-doped alumina.

Most of the creep behaviour of transition metal-doped, polycrystalline alumina at stresses up to 55 $MN\,m^{-2}$ and temperatures between 1375 and 1525° C was slightly non-viscous (i.e. $\dot{\epsilon} \propto \sigma^N$ with $1.03 \leqslant N \leqslant 1.43$) and in accord with previously reported studies [2].

When the range of activation energies and the oxygen partial presure dependencies were taken into account, Hollenberg and Gordon [1] concluded that the steady state creep of transition metal-doped polycrystalline alumina at low stresses ($\sim 5\,MN\,m^{-2}$) was controlled primarily by the lattice diffusion of aluminium ions, either by a vacancy (Ti-doped) or by an interstitialcy (Fe-doped) mechanism. However, due to limited data on grain size effects, it was not possible to evaluate the relative contributions of lattice and grain-boundary diffusion of either the cation or anion to the overall diffusional creep rate. In the present study, the steady state creep behaviour of polycrystalline alumina, pure and doped with iron (0.2 to 2 cation %) and chromium (up to 10 cation %), will be reported over a wide range of grain sizes (6 to 1200 μm). Creep deformation maps will be constructed to illustrate the important diffusional mechanisms which operate and the range of temperatures and grain sizes over which they are dominant.

* Present address: Los Alamos Scientific Laboratory, Los Alamos, New Mexico, USA.

2. Experimental procedure

2.1. Powder preparation

The preparation of high purity (99.999%)* aluminium oxide powder was accomplished by the preparation of aluminium isopropoxide from aluminium metal and its subsequent decompostion by hydrolysis to aluminium hydroxide. Aluminium isopropoxide was prepared by a method similar to that reported by Maxdiyasni *et al.* [3] for the synthesis of yttrium alkoxide. Aluminium metal was reacted at 65 to 75° C with 2-propanol (reagent grade) in the presence of $HgCl_2$ (10^{-4} mol per mol Al) which was used as a catalyst. Two sources of aluminium metal were used.† Distilled, de-ionized water was used for the hydrolysis of the alkoxide. The addition of water to the hot isoproxide solution resulted in a fluffy (unagglomerated) hydroxide powder after the precipitate was filtered and dried. The hydroxide (after drying) was ground, if necessary, and calcined at 1200° C in alumina crucibles to form a fine α-alumina powder. For a thorough description of this organometallic synthesis the reader is referred elsewhere [4].

The dopants (Cr and Fe) were introduced by preparing a slurry of the α-alumina powder in deionized water. This slurry was mixed with another solution containing the dopant metal chloride in solution ($CrCl_3$ or $FeCl_3$). The resulting mixture was then poured into an agitated concentrated solution of ammonium hydroxide leading to the formation of a gel (hydroxide) precipitate. After mixing the oxide–dopant hydroxide very well, it was filtered, dried, and the filter cake was calcined at a temperature sufficiently high to decompose the hydroxide.

2.2. Hot-pressing and annealing

Dense (>98.5% of theoretical) polycrystalline billets were prepared by vacuum hot-pressing at temperatures between 1400 and 1650° C in graphite dies‡ at pressures up to 6000 psi§. The resulting billets were 1.5 in. diameter and ~0.25 in. thick. They were diamond-cut perpendicular to the thickness of the billet to yield 10 to 12 specimens for creep testing. Scanning electron microscope studies with emitted X-rays verified that the dopants were evenly dispersed through the volume of the grains.

Before creep-testing, specimens were usually annealed to establish a range of stable grain sizes. The grain sizes after hot-pressing at 1450° C were 3 to 5 μm for the undoped and chromium-doped material and 15 to 20 μm for the iron-doped samples.¶ All grain sizes are based on 200 to 400 linear intercepts. The average grain size is reported as 1.5 times the intercept average. Annealing was conducted *in vacuo* up to 1900° C (Cr and pure samples) and in air up to 1750° C (Fe doped) to produce a range of grain sizes (6 to 1200 μm). All microstructures were uniform and equiaxed,★ and no exaggerated grain growth was encountered.

After annealing, the specimens were ground and polished with diamond paste (30 μm) to the approximate beam size 2 mm × 5 mm × 30 mm.

2.3 Creep testing

All specimens were tested in four-point dead load tests on a apparatus described in detail elsewhere [1, 5]. Strain rates were calculated from inner load point deflections [6]. Standard equations were used to calculate stresses and strain rates [6]. The testing temperature (1350 to 1550° C) was controlled to ±0.5° C. The oxygen partial pressure was maintained with various gas mixtures (Air–N_2, CO–CO_2) and measured with a solid state galvanic cell (ZrO_2 + CaO). Creep strains were normally less than 1 or 2%.

3. Results and discussion

3.1. Stress dependence of steady state creep rate

A major objective of this study was the documentation of the dependence of the steady state creep rate of pure and doped polycrystalline alumina over a wide range of experimental conditions (tem-

* Verified by semiquantitative emission spectrographic analysis.

† A. D. MaKay Inc., aluminium pellets; Aluminum Company of America, piglet aluminium.

‡ Poco HPD-1 and HPD-3

§ 1 psi = 1.450 × 10^{-4} N m^{-2}

¶ 5 to 7 μm for hot-pressing at 1300° C

★ A few tabular or straight sided grains were observed in the iron-doped specimens. However, the grain size distributions were uniform

peratures, grain sizes, dopant levels and atmospheres). Experimental conditons were varied in an effort to distinguish creep regimes in which viscous (i.e. $\dot{\epsilon} \propto \sigma^N$, $N = 1$), slightly non-viscous ($N = 1.1$ to 1.7), and non-viscous ($N > 1.7$) behaviour was dominant.

Reports of slightly non-viscous creep of polycrystalline alumina abound in the literature. Heuer *et al.* [2] were the first investigators to document this behaviour. They reported stress exponents N between 1.08 and 1.67 for bending tests on pure and MgO-doped alumina ($1.8 <$ grain size < 16.5 μm, $1300 \leqslant T \leqslant 1700^\circ$ C) at stresses between 7 and 211 MN m^{-2}. These authors also re-analyzed the earlier work of Folweiler [7], and Warhsaw and Norton [8], and concluded that stress exponents ranging between 1.07 and 1.7 were more representative of the creep data than viscous behaviour ($N = 1$). Later Cannon [9] (21 to 51 μm) and Sugita and Pask [10] (4.5 to 10.5 μm) reported slightly non-viscous behaviour ($N = 1.1$ to 1.3) for the compression creep-testing of MgO-doped polycrystalline alumina. Apparently stress exponents up to 1.7 are characteristic of creep deformation in bending and compression of polycrystalline alumina, pure and doped, over a wide range of experimental conditons.

A summary of stress exponents measured* in this study and those reported by Hollenberg and Gordon [1] is given in Table I. In general, nearly all of the creep data are characterized by slightly non-viscous creep behaviour with stress exponents that vary between 1.03 and 1.43 for grain sizes between approximately 6 and 110 μm. An interesting and notable exception of viscous creep ($N = 1$) was observed for the creep of polycrystalline alumina doped with 2% iron and creep-tested in a reducing atmosphere. Viscous creep behaviour is clearly shown in Fig. 1 for tests at 1250 and 1450° C. Deflection rate versus load data which were plotted on linear scales resulted in straight lines that passed through the origin, a definitive tests for viscous behaviour.

Larger stress exponents (1.4 to 1.8) were found in creep tests at 1450° C in pure and chromium-doped specimens with larger grain sizes (70 to 306 μm). When similar specimens were tested at higher temperatures (1550° C), significantly non-viscous behaviour ($N = 2.3$ to 2.9) was encountered and is similar to that reported earlier in the literature [8, 11–13].

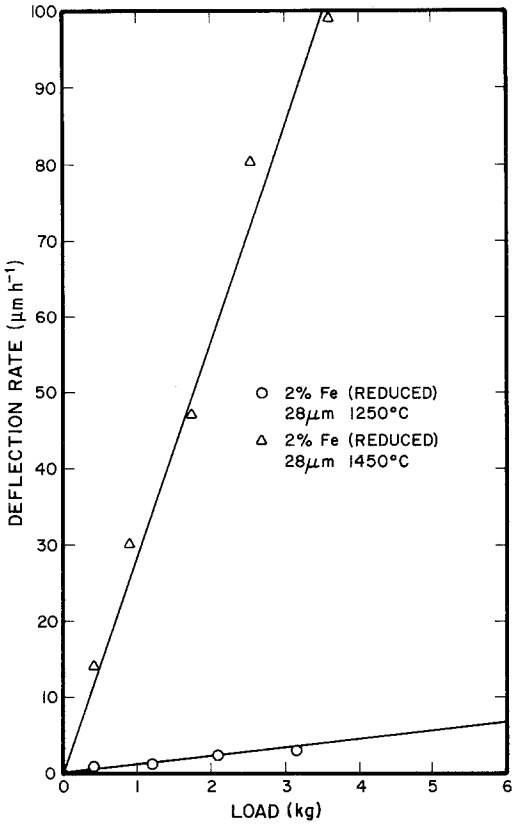

Figure 1 Viscous creep of polycrystalline alumina doped with 2% cation iron at $P_{O_2} \cong 10^{-6}$ atm.

3.2. Grain size dependencies: pure and chromium-doped alumina

Creep experiments were designed to isolate the effect of grain size on the steady state creep rate. Parameters such as temperature, stress, dopant concentration, P_{O_2}, and even hot-pressing billet (density, etc) were maintained constant for a series of tests. The grain size was varied by annealing samples at temperatures higher than the test temperature to establish a range of stable grain sizes.

Experiments were conducted on pure and chromium-doped alumina (1.0 and 10.0 cation %) as a function of grain size (GS). A stress of 5 MN m^{-2} and an air atmosphere were used. The results of these dead load experiments are given in Fig. 2. Chromium additions up to 10% had little or no effect on the creep rate of polycrystalline alumina for grain sizes between 6 and 70 μm in accord with the earlier work of Hollenberg and Gordon [1]. Least squares analyses of the data revealed grain-size exponents $m(\dot{\epsilon} \propto (\mathrm{GS})^{-m})$ of 1.80 for pure

* Normally determined by measuring the steady state strain rate at various stresses on the same creep specimen.

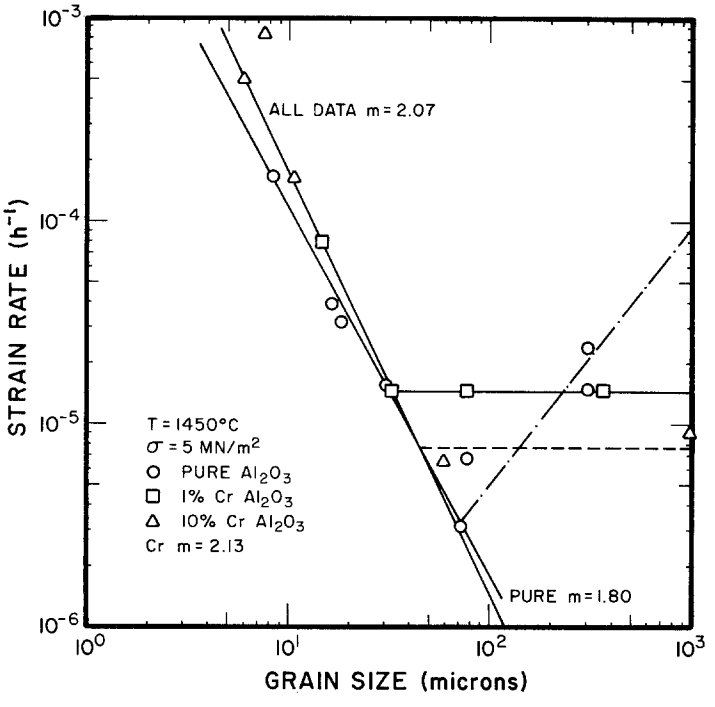

Figure 2 Grain size effects on the steady state creep of pure and chromium-doped polycrystalline alumina.

TABLE I Strain rate–stress exponents (N) in polycrystalline alumina

Composition (cation %)	N	Grain size (μm)	Temperature (°C)	Stress (MN m^{-2})	P_{O_2} (atm)	Number of Specimens
Undoped	1.30 ± 0.15	9–72	1450	4–50	0.86	5
Undoped	1.76	76	1450	3–30	0.18	1
Undoped	1.40	306	1450	4–10	0.18	1
Undoped	2.88	306	1550	4–10	0.18	1
Undoped	2.33	306	1550	4–20	0.18	1
1% Cr[a]	1.30	9	1400–1550	5–55	0.86	2
1% Cr	1.03	15	1450	4–50	0.86	1
1% Cr	1.21	32	1450	4–50	0.86	1
1% Cr	1.43	77	1450	4–32	0.86	1
1% Cr	1.67	276	1450	4–9	0.86	1
10% Cr	1.15 ± 0.04	6	1450	4–40	10^{-9}	2
10% Cr	1.11	29	1450	4–10	10^{-9}	1
10% Cr	1.48	60	1450	4–20	0.86	1
10% Cr	2.38	1200	1550	8–29	0.86	1
0.2% Fe[a]	1.14 ± 0.06	15	1400–1500	1–10	0.86	3
0.2% Fe	1.14	27–38	1450	4–50	0.86	2
1.0% Fe[a]	1.0	15	1500	1–15	0.86	1
1.0% Fe	1.25 ± 0.06	26–107	1450	4–50	0.86	3
1.0% Fe[a]	1.25 ± 0.05	42	1400–1500	5–55	0.86	1
1.0% Fe[a]	1.0	15	1500	1–10	6.31×10^{-3}	1
1.0% Fe	1.29	38	1450	4–50	10^{-8}	1
2.0% Fe	1.05	28	1450	4–36	$\sim 10^{-6}$	1
2.0% Fe	1.03	28	1450	4–34	$\sim 10^{-6}$	1
2.0% Fe	0.90	28	1250	4–30	$\sim 10^{-6}$	1
1/2% Ti[a]	1.07	63	1525	1–10	0.86	1
1/2% Ti[a]	1.07	63	1525	3–30	10^{-9}	1

[a]Data taken from [1]

Al_2O_3, 2.13 for both the 1 and 10% Cr specimens combined, and 2.07 for all the pure and chromium-doped materials combined. These data are consistent with the interpretation that the steady state creep rate is controlled by a cation lattice diffusion process (i.e. Nabarro–Herring creep).

The dead-load creep characteristics of coarse grained (40 to 1200 μm) polycrystalline alumina, pure and doped with chromium are also shown in Fig. 2. When the grain size exceeded 40 to 70 μm, the steady state creep rate was no longer reciprocally related to the grain size. In undoped material the creep rate actually increased with grain sizes over 70 μm. In chromium-doped alumina the creep rate was independent of the grain size for grain sizes over 40 to 60 μm. In this grain size independent regime the creep rate decreased with an increase in chromium concentration from 1 to 10% indicating a possible hardening effect.

In the regime of large grain sizes non-viscous creep was much more dominant. The stress exponents at small grain sizes (i.e. $\dot{\epsilon} \propto (GS)^{-2}$) increased from 1.03 to 1.30 to 1.4 to 2.9 in the large grain size limit (i.e. $\dot{\epsilon} \propto (GS)^m$, $m = 2$ (pure); $m = 0$ (chromium)). Furthermore, the stress exponents in the large grain size regime were found to be dependent on the temperature. They increased from 1.4 to 1.8 at 1450° C to 2.3 to 2.9 at 1550° C. Due to a change in mechanism the activation energy also changed with temperature. At 1450° C the activation energy was ~60 kcal mol^{-1} (undoped alumina) while at 1575° C, the activation energy increased to approximately 100 kcal mol^{-1}. Power law creep ($N \sim 3$ to 4) has been well documented in previous work on the creep of polycrystalline alumina at temperatures over 1600° C [8, 11–13]. Evidently a transition in mechanism occurs over a range of temperatures (1450 to 1550° C) from slightly non-viscous behaviour (1.4 to 1.8) to definite non-viscous power law creep ($N \sim 3$). It is possible that recovery processes such as discolation climb become important in non-viscous creep at elevated temperatures. These may be responsible for the increase in stress exponents to values around 3 at 1550° C.

3.3. Grain size dependencies: iron-doped alumina

Extensive creep tests were conducted over a wide range of grain sizes in both oxidizing and reducing atmospheres on polycrystalline alumina doped with 0.2, 1.0, and 2.0 cation % iron. The effects of doping with iron are illustrated in Fig. 3 for creep tests conducted at 1450° C at a stress of 5 MN m^{-2}. In creep tests conducted in air and in reducing atmospheres (~10^{-6} atm), it is expected that a significant fraction of the iron is present as a divalent ion in substitutional solid solution for aluminium. Additions of 0.2, 1.0, and 2.0 cation % iron enhanced the creep rate of polycrystalline alumina by factors of ~2, ~7, and ~18 respectively. Reducing the oxygen partial pressure from 0.86 to 4.66×10^{-7} atm increased further the creep rate of the specimens doped with 2% Fe. All of these results, in combination with the effects of P_{O_2} reported earlier by Hollenberg and Gordon [1], indicate that divalent iron enhances the diffusional creep rate of polycrystalline alumina.

Gordon [14] has predicted for the system Al_2O_3–Fe_2O_3–FeO in the limit of a large grain size and/or a high value of the aluminium ion lattice diffusivity (D^l_{Al}), that the diffusional creep rates in the low stress regime will be controlled by oxygen grain-boundary diffusion (because cation lattice diffusion becomes too rapid). Aluminium lattice diffusion can be enhanced by increasing the iron dopant level and/or reducing the oxygen partial pressure. Both of these changes will increase the concentration of divalent iron leading to enhanced lattice diffusion via aluminium ion interstitials.

Verification of Gordon's predictions are shown in Fig. 3. Doping with 1% Fe not only increased the creep rate in air but also modified the grain-size exponent m of ~2 to 2.34. An exponent of 2.34 is intermediate so that expected by the Nabarro–Herring ($m = 2$) and Coble ($m = 3$) theories for lattice and grain boundary diffusion control of the creep rate. Using a procedure developed by Gordon and Hodge [15] for the creep of polycrystalline magnesium oxide, aluminium lattice (D^l_{Al}) and oxygen grain-boundary ($\delta_O D^b_O$) diffusion coefficients can be extracted from the creep data. When both cation lattice and anion grain-boundary diffusion contribute to the overall creep rate, the respective diffusion coefficients can be computed from the following equation [14]

$$\dot{\epsilon} = \frac{44\Omega_v \sigma}{2\pi kT (GS)^2} D^l_{Al} \Big/ \left[1 + \frac{3}{2} \frac{(GS) D^l_{Al}}{\pi \delta_O D^b_O}\right] \quad (1)$$

Under these conditions, the creep rate will exhibit a mixed grain-size dependence ($2 < m < 3$).

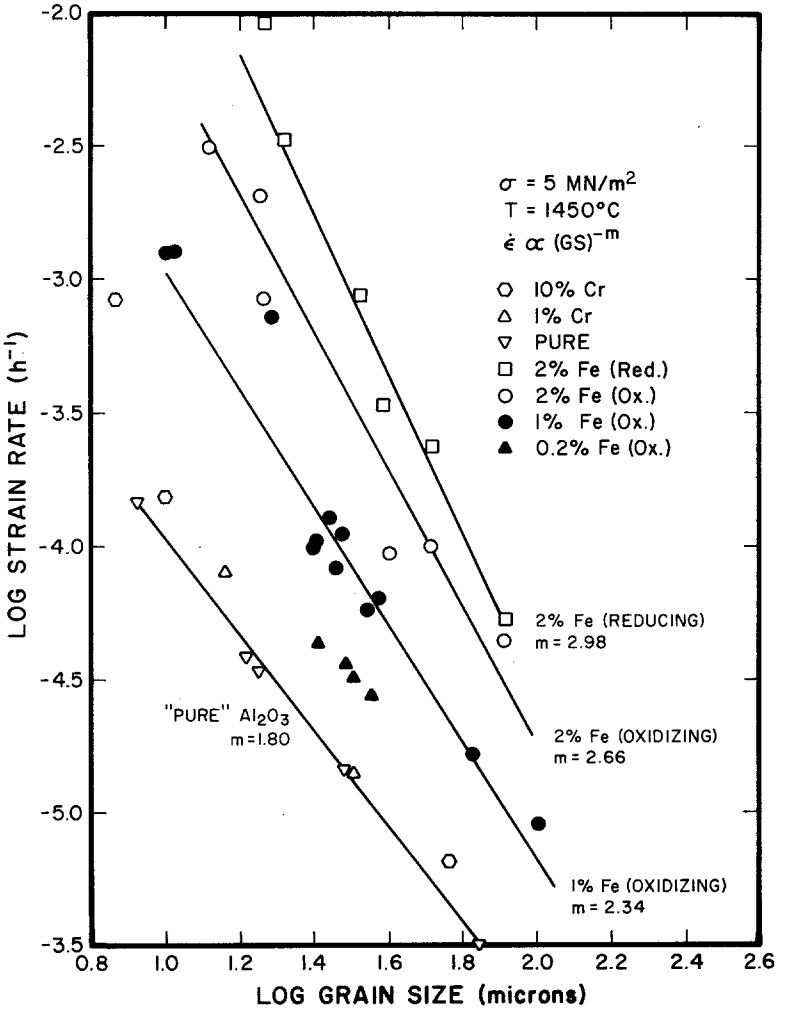

Figure 3 Grain size and impurity effects on the creep of polycrystalline alumina.

Equation 1 can be rewritten in the form

$$\dot{\epsilon}(GS)^2 = -\frac{3}{2\pi}\frac{D^l_{Al}}{\delta_O D^b_O}\dot{\epsilon}(GS)^3 + \frac{44}{\pi}\frac{\Omega_v \sigma}{kT}\frac{D^l_{Al}}{2} \quad (2)$$

In Equations 1 and 2 Ω_v is the molecular volume of Al_2O_3, σ is the stress, GS is the grain size, T is the absolute temperature, k is Boltzmann's constant, D^l_{Al} is the aluminium lattice diffusion coefficient, D^b_0 is the oxygen grain-boundary diffusion coefficient, and δ_0 is the effective grain boundary thickness for oxygen grain-boundary diffusion. Referring to Equation 2, a plot of $\dot{\epsilon}(GS)^2$ versus $\dot{\epsilon}$ $(GS)^3$ yields a line of slope equal to $-\left[\frac{3}{2\pi}\frac{D^l_{Al}}{\delta_O D^b_O}\right]$ and intercept equal to $\frac{44}{\pi}\left[\frac{\Omega_v \sigma D^l_{Al}}{kT2}\right]$.

Using predicted points from the least-squares line in Fig. 3, values for D^l_{Al} (6.72×10^{-12} cm^2 sec^{-1}) and $\delta_0 D^b_0$ (2.10×10^{-14} cm^3 sec^{-1}) were calculated for polycrystalline alumina doped with 1% Fe (equilibrated in an air atmosphere).

By doping at even higher concentrations (i.e. 2 cation % Fe) and reducing the oxygen partial pressure (4.66×10^{-7} atm) D^l_{Al} can be increased even further. (At 1450° C no second phase precipitation was observed in the reduced specimens.) If ambipolar diffusional creep theory is correct, these changes should lead to larger grain size exponents m and creep rates controlled more and more by oxygen grain-boundary transport. As indicated in Fig. 3, doping with 2% Fe and creep-testing in air resulted in higher strain rates and a larger grain-size exponent ($m = 2.66$). When creep tests were conducted in a reducing atmosphere (P_{O_2} = 4.66×10^{-7} atm), creep rates increased even further, the relative increase was smaller at large

TABLE II Aluminium lattice and oxygen grain-boundary diffusivities (1450° C) in iron-doped polycrystalline alumina

P_{O_2} (atm)	Cation % Fe	D^l_{Al} ($cm^2\ sec^{-1}$)	$\delta_O D^b_O$ ($cm^3\ sec^{-1}$)	m
0.18	0*	6.9×10^{-13}	–	~2
0.18	0.2*	1.7×10^{-12}	–	~2
0.18	1.0†	6.7×10^{-12}	2.1×10^{-14}	2.34
0.18	2.0†	5.0×10^{-11}	4.1×10^{-14}	2.66
4.66×10^{-7}	2.0‡	–	5.9×10^{-14}	2.98
Tracer (Extrapolated)§		1.0 N 10;13		

* Calculated from Nabarro–Herring creep equation modified for an ionic compound [14]
† Calculated from a procedure similar to that reported by Gordon [14] and Gordon and Hodge [15]
‡ Calculated from Coble creep equation modified for an ionic compound [14]
§ From [17]

grain sizes than in fine-trained material. Under these conditions the creep grain size exponent was 2.98, its largest value and in excellent agreement with that predicted by Coble creep.

In Table II, a summary is given for values of D^l_{Al} and $\delta_O D^b_O$ computed from creep data at the 0.0, 0.2, 1.0 and 2.0% dopant concentrations. The data in Table III indicate that both D^l_{Al} and $\delta_O D^b_O$ increase with iron doping, in particular the concentration of divalent iron. In addition as D^l_{Al} increases the relative contribution of oxygen grain-boundary diffusion increases giving rise to increasing values of the creep rate–grain size exponent. Both of these effects are in accord with that predicted by ambipolar diffusional creep theory [14, 16].

Finally, it is interesting to note that when the creep process is rate-controlled by oxygen grain-boundary diffusion (2% Fe-reducing atmosphere), the creep rate is linear with the stress (viscous creep). Since the creep of polycrystalline alumina is normally slightly non-viscous when there is a contribution of both cation lattice and anion grain-boundary diffusion (Table I), there is an indication that the non-viscous behaviour is associated with the bulk diffusion of the cation. Slightly non-viscous stress exponents may be due to interfacial effects whereby grain boundaries do not act as perfect vacancy sinks [4, 18, 19].

3.4. Activation energies for the creep of polycrystalline alumina

Creep activation energies were determined from temperature change experiments (1350 to 1525° C)

TABLE III Summary of creep activation energies for polycrystalline alumina, pure and doped with transition metal impurities

Dopant (Cation %)	No. of specimens	Activation energy (kcal mol^{-1})	Grain size (μm)	Grain-size exponent m
Undoped	2	130 ± 5	18	1.80
1% Cr	1	124	15	~2
1% Cr	1	129	30	~2
0.2% Fe	1	134	25	~2
1% Fe	1	115	15	2.34
1% Fe*	1	143	15	–
1% Fe	1	125	32	2.34
1% Fe	1	117	66	2.34
1% Fe	1	117	107	2.34
2% Fe (Reducing)	1	119	81	2.98
0.25 Ti–0.25 Mn†	1	100	24	4.4
0.25 Ti–0.25 Cu†	1	94	15	>3

* From earlier work by Hollenberg and Gordon [1]
† Viscous creep controlled by oxygen grain-boundary diffusion [4]

on pure, chromium-doped, and iron-doped polycrystalline alumina. A summary of all activation energies is given in Table III. An activation energy of approximately 129 kcal mol^{-1}, is characteristic of deformation in pure and chromium-doped alumina. For the specimens doped with 1 cation % Fe, in which the deformation mode was a mixture of both aluminium lattice and oxygen grain boundary diffusion, values ranged between 143 kcal mol^{-1} to a lower limit of 117 kcal mol^{-1}. Finally activation energies for specimens in which the deformation mode was controlled entirely by oxygen grain-boundary diffusion were approximately 94 to 119 kcal mol^{-1} on the low end of the experimental range.

In the diffusional creep of a polycrystalline ceramic in which cation lattice diffusion is comparable to anion grain-boundary diffusion (e.g. 1% Fe in air), the apparent creep activation energy is expected to vary both with temperature and grain size because of the dependence between the complex diffusion coefficient ($D_{complex}$), the grain size (GS), the cation lattice diffusion coefficient, and the anion grain boundary diffusion coefficient according to the following relations;

$$\dot{\epsilon} = \frac{44\Omega_v \sigma}{kT(GS)^3} D_{complex} \quad (3)$$

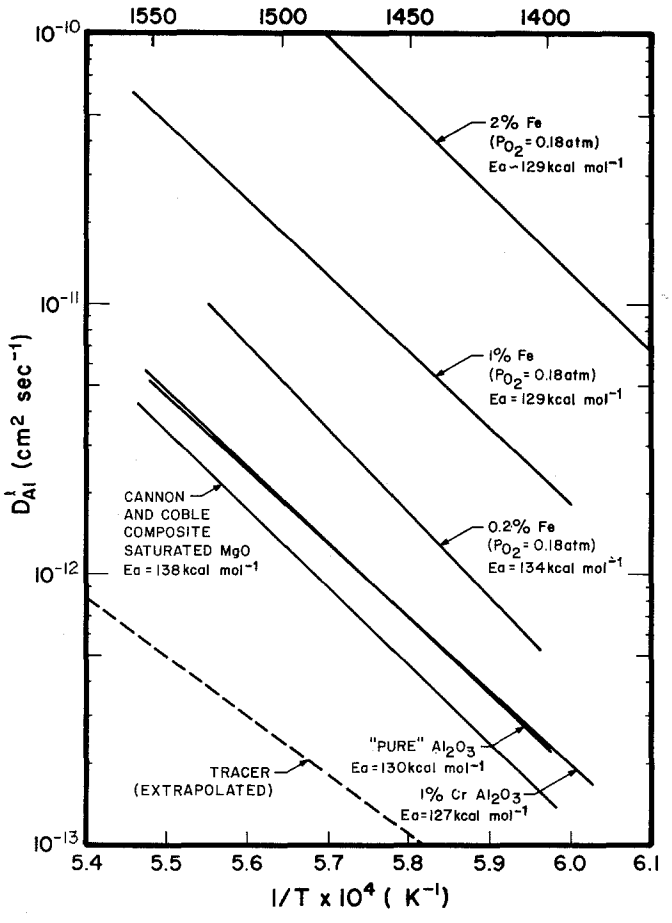

Figure 4 Calculated aluminium lattice diffusion coefficients.

$$D_{\text{complex}} = \frac{1}{2}\left[\frac{(GS)}{\pi} D^{l}_{Al}\right] \Big/ \left[1 + \frac{3}{2}\frac{(GS)}{\pi}\frac{D^{l}_{Al}}{\delta_O D^{b}_{O}}\right] \quad (4)$$

If, activation energies of 150 and 105 kcal mol^{-1} are assigned, respectively, to aluminium lattice diffusion and oxygen grain-boundary diffusion in iron-doped alumina,* then the apparent activation energy (using computer calculations) at 1450° C would vary between 140 kcal mol^{-1} at a grain size of 16 μm to 120 kcal mol^{-1} at a grain size of ~120 μm. This range is comparable to that observed experimentally. The highest activation (~150 kcal mol^{-1}) energy would be expected in fine-grained samples (<1 μm) tested at low temperatures (~1200° C), while the lowest activation energy would occur in large grain-size (>120 μm) material tested at high temperatures (>1600° C). When one considers that creep activation energies have an experimental uncertainty of ±10 kcal mol^{-1}, a maximum variation in the apparent activation energy of approximately 20 kcal mol^{-1} would be difficult to distinguish in the realm of experimental grain sizes (6 to 110 μm) and temperatures where dead-load creep rates are readily measured (1400 to 1600° C).

3.5. Estimation of diffusion coefficients from diffusional creep data

Aluminium lattice diffusion coefficients in polycrystalline alumina, pure and doped with chromium and iron are plotted at various temperatures in Fig. 4 using the data in Tables II and III. In all cases, the diffusion coefficients are larger than those obtained from an extrapolation of aluminium tracer values [14] at higher temperatures. It should be noted that all computations of diffusivities were made using creep data in the limit of low stress (5 MN m^{-2}). Consequently, it is not likely that the diffusivities are over-estimated because of the slightly non-viscous behaviour which becomes an important factor at higher stress

* These are highest and lowest values that might be expected for aluminium lattice and oxygen grain-boundary diffusion

levels. The effect of iron-doping on cation lattice diffusion is readily apparent. Nearly two orders of magnitude (~70X) separate the diffusion coefficients for pure alumina and material doped with 2% Fe.

Also included in Fig. 4 are values of D^{l}_{Al} computed from the viscous creep of polycrystalline alumina saturated with MgO. In a composite analysis of eight different creep studies, Cannon and Coble [19] report that all the data fall within a factor of two of the following expression:

$$D^{l}_{Al} = 1.36 \times 10^{5} \exp(-138\,000/RT)\,\mathrm{cm}^2\,\mathrm{sec}^{-1}$$

These values are in reasonable agreement with the values estimated from the undoped and chromium-doped specimens from this study.

As the concentration of cation lattice defects increases by doping with divalent iron, cation lattice diffusion increases to a level at which it is too fast to be rate-controlling. At this stage, the creep rate becomes rate-limited by oxygen grain-boundary diffusion. Estimates of $\delta_O D^{b}_{O}$ inferred from the creep of polycrystalline alumina doped with 1% Fe (oxidizing), and 2% Fe (oxidizing and reducing) are shown in Fig. 5. Data for $\delta_{Al} D^{b}_{Al} = 8.6 \times 10^{-4} \exp(-100\,000/RT)\,\mathrm{cm}^3\,\mathrm{sec}^{-1}$, which were computed by Cannon and Coble [19] from creep data on fine-grained ($<10\,\mu$m) Al_2O_3 (pure and doped with MgO) at low temperatures, and values of $\delta_O D^{b}_{O}$ inferred from abnormal grain growth and oxygen self diffusion in pure alumina [20] are also included in Fig. 5 for comparison. It is clear from these data that oxygen grain-boundary diffusion in doped polycrystalline alumina is over three orders of magnitude larger than that in undoped material, and over two orders of magnitude larger than aluminium grain-boundary diffusion in MgO-doped alumina. Doping alumina with Fe^{2+} gives rise to a considerable enhancement in the oxygen grain-boundary diffusivity.

3.6. Creep deformation mechanism maps

Mapping of creep deformation modes for polycrystalline materials has received renewed interest

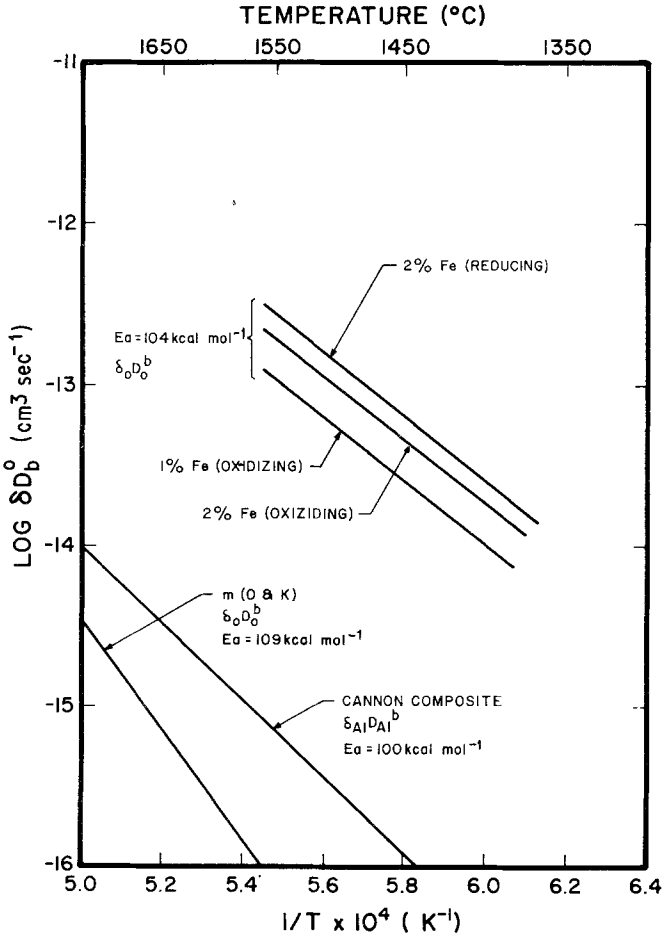

Figure 5 Estimates of oxygen and aluminium grain-boundary diffusivities in polycrystalline alumina.

with the work of Ashby [21] in which lines of constant strain rate (iso-strain rate lines) are computed for variable stresses and temperatures at a fixed grain size. Transitions between viscous and non-viscous creep regimes can be readily identified in maps of this type. Recently Langdon [22] proposed a deformation map in which iso-strain rate lines are computed for variable stresses and grain sizes at a fixed temperature. This map is particularly useful for materials in which diffusional creep modes are important since they are very grain-size dependent. Another map which is useful for diffusional creep regimes consists of iso-strain rate lines computed with variable temperatures and grain sizes at a fixed level of stress [23].

Two maps of this latter type have been constructed for the diffusional creep of polycrystalline alumina doped with 1 and 2 cation % iron. In these materials, three diffusional mechanisms can be expected to operate. At very small grain sizes and low temperatures creep rates will be dominated by aluminium grain-boundary diffusion according to

$$\dot{\epsilon} = \frac{44\Omega_v\sigma}{kT(GS)^3}\,\frac{\delta_{Al}D^b_{Al}}{2}. \qquad (5)$$

At larger grain sizes and higher temperatures, creep rates will be governed by a competition between aluminium lattice and oxygen grain-boundary diffusion according to Equation 1.

TABLE IV Input data for the creep deformation maps in iron-doped polycrystalline alumina

Coble (aluminium grain-boundary diffusion)*

$\delta_{Al}D^b_{Al} = 8.6 \times 10^{-4} \exp(-100\,000/RT)\text{cm}^3\,\text{sec}^{-1}$ (in Equation 5)

Nabarro–Herring (aluminium lattice diffusion) and Coble (oxygen grain-bounady diffusion) (for use in Equation 1)

$D^l_{Al}(1\%\,\text{Fe}) = 7.15 \times 10^{7} \exp(-150\,000/RT)\text{cm}^2\,\text{sec}^{-1}$

$\delta_0 D^b_O(1\%\,\text{Fe}) = 4.38 \times 10^{-1} \exp(-105\,000/RT)\text{cm}^3\,\text{sec}^{-1}$

$D^l_{Al}(2\%\,\text{Fe}) = 5.26 \times 10^{8} \exp(-150\,000/RT)\,\text{cm}^2\,\text{sec}^{-2}$

$\delta_0 D^b_O(2\%\text{Fe}) = 8.48 \times 10^{-1} \exp(-105\,000/RT)\text{cm}^3\,\text{sec}^{-1}$

* Taken from measurements on polycrystalline alumina saturated with MgO [19] and assumed, as a first approximation, to be valid in iron-doped material.

The effect of doping polycrystalline alumina with a variable valent ($Fe^{2+} - Fe^{3+}$) impurity is shown for two dopant levels (1 and 2 cation %) in Figs. 6 and 7. The input data for these two deformation maps are summarized in Table IV. The Coble creep regime at low temperatures and small grain sizes was based on Cannon and Coble's evaluation [19] of $\delta_{Al}D^b_{Al}$ for MgO-doped alumina. Most of the observed creep behaviour was a mixture of two mechanisms: (1) Nabarro–Herring creep controlled by aluminium lattice diffusion and (2) Coble creep controlled by oxygen grain-boundary diffusion.

At the 1% dopant level and a low stress of

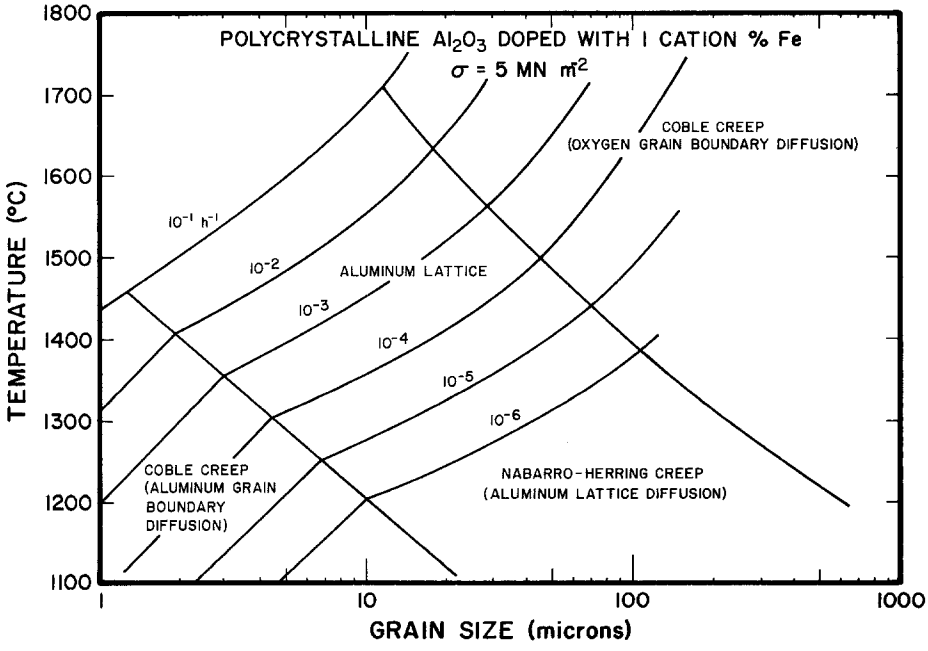

Figure 6 Deformation map at constant stress for polycrystalline alumina doped with 1 cation % iron.

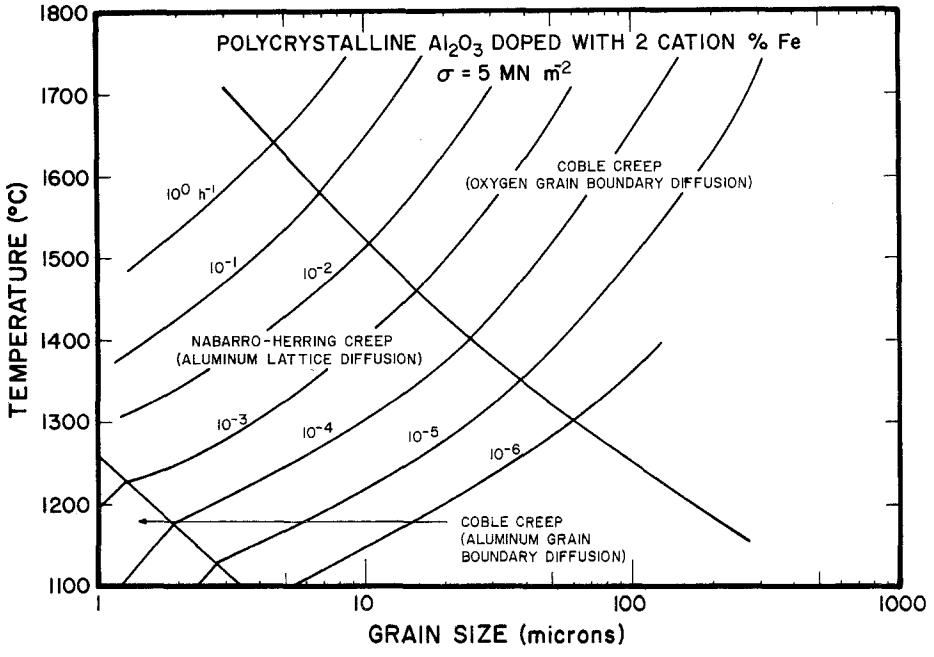

Figure 7 Deformation map at constant stress for polycrystalline alumina doped with 2 cation % iron.

5 MN m^{-2}, three diffusional creep mechanisms can operate. For small grain sizes ($<10\,\mu$m) and low temperatures ($<1300^\circ$ C) Coble creep, which is rate-limited by aluminium grain-boundary diffusion, is predicted to be dominant. At higher temperatures and larger grain sizes, an extremely broad range exists where both aluminium lattice and oxygen grain-boundary diffusion are coupled. It is noted that transitions between different deformation regimes are indicated on the creep maps by single lines. It is to be emphasized that these lines represent situations where the creep rates of the two processes in question are equal. It must be remembered that in the vicinity of the boundaries deformation modes are mixed. In particular, mixed modes of deformation may exist in diffusional creep regimes over several orders of magnitude in strain rate.

Because aluminium lattice diffusion is enhanced by doping with divalent iron, oxygen grain-boundary diffusion gradually becomes the rate-limiting step. This effect can be seen by referring to the map for the 2% dopant (Fig. 7). Aluminium lattice diffusion has increased to the point that Coble creep controlled by aluminium grain-boundary diffusion is almost non-existent. Furthermore, the influence of oxygen grain-boundary diffusion as the rate-determining process has shifted to lower temperatures and smaller grain sizes. Figs. 6 and 7 represent deformation maps for creep tests in an oxidizing atmosphere. When creep tests at the 2% dopant were conducted in a reducing environment ($P_{O_2} \sim 10^{-6}$ atm), the deformation process was completely dominated by oxygen grain-boundary diffusion at 1450° C for grain sizes between 18 and 83 μm. Thus the transition between Nabarro–Herring (aluminium lattice diffusion) and Coble (oxygen grain-boundary diffusion) creep shifted to even lower temperatures and smaller grain sizes. This shift is due to an increase in cation lattice diffusion relative to anion grain-boundary diffusion.

The creep maps for undoped and chromium-doped alumina would be similar to that shown in Fig. 6 for the 1% dopant level except that the transition regions between (1) aluminium grain boundary and aluminium lattice diffusion and (2) aluminium lattice and oxygen grain-boundary diffusion would be shifted to higher temperatures and larger grain sizes. The Nabarro–Herring regime controlled by aluminium lattice diffusion would be dominant for the grain size range which was investigated in this study (6 to 70 μm). Coble creep which is rate limited by aluminium grain-boundary diffusion would be expected to dominate at grain sizes below 6 to 10 μm. Coble creep which is rate-limited by oxygen grain-boundary diffusion is only seen when aluminium lattice diffusion is

significantly enhanced (e.g. doping with divalent iron).

Finally the maps in Figs. 6 and 7 were constructed for a low stress (5 MN m^{-2}) where viscous creep is expected to be dominant. At larger stresses and grain sizes over $\sim 100\,\mu$m non-viscous creep modes can be expected to become important.

The nature of anion–cation ambipolar coupling is illustrated in the deformation maps depicted in Figs. 6 and 7. Two regimes of Coble creep are possible in an oxide where oxygen grain-boundary transport is rapid: (1) aluminium grain-boundary diffusion control at low temperatures and small grain sizes and (2) oxygen grain-boundary diffusion control at high temperatures and large grain sizes.

4. Summary

The steady state creep of polycrystalline alumina, pure and doped with chromium, at low stresses is rate limited primarily by the lattice diffusion of aluminium ions and independent of chromium concentration. Doping alumina with divalent iron (Fe^{2+}) in solid solution enhances the lattice diffusion of aluminium ions. The steady state creep of iron-doped alumina is mixed in character in that both aluminium lattice and oxygen grain-boundary diffusion are comparable in magnitude. At high concentrations of divalent iron (i.e. high iron dopant levels and low oxygen partial pressures) aluminium lattice diffusion is too rapid to be rate-limiting. Under these conditions, viscous Coble creep which is rate-limited by oxygen grain-boundary diffusion is dominant. Construction of creep deformation mechanism maps revealed the presence of two regimes of Coble creep: one controlled by aluminium grain-boundary diffusion at low temperatures and small grain sizes and the other controlled by oxygen grain-boundary diffusion at high temperatures and larger grain sizes. At very large grain sizes ($>100\,\mu$m) and high stresses non-viscous creep begins to become important and creep rates either increase (undoped) or do not change (chromium-doped) as the grain size is increased. In this limit, chromium additions significantly depress the steady state creep rate.

Acknowledgements

The authors are grateful for helpful discussions with J. D. Hodge. This research was supported by the Energy Research and Development Administration under Contract E(11-1)-1591.

References

1. GLENN W. HOLLENBERG and RONALD S. GORDON, *J. Amer. Ceram. Soc.* **56** (3) (1973) 140.
2. A. H. HEUER, R. M. CANNON, and N. J. TIGHE, "Ultrafine-Grain Ceramics", edited by J. J. Burke, N. L. Need, and Volker Weiss, (Syracuse University Press, Syracuse, 1970) p. 339.
3. K. S. MAZDIYASNI, C. T. LYNCH, and J. S. SMITH, *Inorg. Chem.* **5** (1966) 342.
4. PAUL A. LESSING, Ph.D. Thesis, Univeristy of Utah, (1976).
5. G. W. HOLLENBERG, Ph.D. Thesis, University of Utah, (1972).
6. G. W. HOLLENBERG, G. R. TERWILLIGER, and R. S. GORDON, *J. Amer. Ceram. Soc.* **54** (4) (1971) 196.
7. R. C. FOLWEILER, *J. Appl. Phys.* **32** (1961) 773.
8. S. I. WARSHAW and F. H. NORTON, *J. Amer. Ceram. Soc.* **45** (1962) 479.
9. W. R. CANNON, Ph.D. Thesis, Stanford University, (1971).
10. TADOAKI SUGITA and J. A. PASK, *J. Amer. Ceram. Soc.* **53** (1970) 609.
11. W. R. CANNON and O. D. SHERBY, *ibid* **56** (1973) 157.
12. R. L. COBLE and Y. H. GUERARD, *ibid* **46** (1963) 353.
13. G. V. ENGLEHARDT and F. THUMLER, *Ber. Dt. Keram. Ges.* **47** (1970) 571.
14. R. S. GORDON, in "Mass Transport Phenomena in Ceramics", edited by A. R. Cooper and A. H. Heuer, (Plenum Press, New York, (1975) 445.
15. R. S. GORDON and J. D. HODGE, *J. Mater. Sci.* **10** (1975) 200.
16. RONALD S. GORDON, *J. Amer. Ceram. Soc.* **56** (3) (1973) 147.
17. A. E. PALADINO and W. D. KINGERY, *J. Chem. Phys.* **37** (1962) 957.
18. R. M. CANNON, Ph.D. Thesis, MIT, (1975).
19. R. M. CANNON and R. L. COBLE, in "Deformation of Ceramic Materials", edited by R. C. Bradt and R. E. Tressler, (Plenum Press, New York, 1975) 61.
20. R. E. MISTLER, Sc.D. Thesis, MIT (1967).
21. M. F. ASHBY, *Acta Met.* **20** (1972) 887.
22. T. G. LANGDON, "Grain Boundary Deformation Processes" in "Deformation of Ceramic Materials", edited by R. C. Bradt and R. E. Tressler (Plenum Press, New York 1975) 101.
23. J. D. HODGE, P. A. LESSING and R. S. GORDON, *J. Mater. Sci.*

Received 7 January and accepted 22 February 1977.